Magnetic properties of single-crystalline $CeCuGa_3$

Devang A. Joshi,[1] P. Burger,[1] P. Adelmann,[1] D. Ernst,[1] T. Wolf,[1] K. Sparta,[2] G. Roth,[2] K. Grube,[1] C. Meingast,[1] and H. v. Löhneysen[1,3]

[1]*Institut für Festkörperphysik, Karlsruhe Institute of Technology, D-76021 Karlsruhe, Germany*

[2]*Institute of Crystallography, Rheinisch-Westfälische Technische Hochschule (RWTH) Aachen, Jägerstrasse 17/19, D-52056 Aachen, Germany*

[3]*Physikalisches Institut, Karlsruhe Institute of Technology, D-76031 Karlsruhe, Germany*

(Received 19 April 2012; published 25 July 2012)

The magnetic behavior of single-crystalline $CeCuGa_3$ has been investigated. The compound forms in a tetragonal $BaAl_4$-type structure consisting of rare-earth planes separated by site-disordered Cu-Ga layers. If the Cu-Ga site disorder is reduced, $CeCuGa_3$ adopts the related, likewise tetragonal, $BaNiSn_3$-type structure, in which the inversion symmetry is lost. We report on a detailed study of single crystals with the centrosymmetric structure variant which exhibit ferromagnetic order below $\approx$4 K with a strong, planar anisotropy. The magnetic behavior above the transition temperature can be well understood by the crystal-field splitting of the $4f$ Hund's rule ground-state multiplet $^2F_{5/2}$ of Ce^{3+}.

DOI: 10.1103/PhysRevB.86.035144 PACS number(s): 75.50.Cc, 75.30.Gw, 75.30.Mb

I. INTRODUCTION

Rare-earth intermetallic compounds containing Ce have attracted considerable attention due to their diverse properties, including valence fluctuations, heavy-fermion behavior, and different types of magnetic ordering. The variety of different ground states arises due to the interaction of $4f$ electrons with the crystal electric field, and the competition between intersite Ruderman-Kittel-Kasuya-Yosida and on-site Kondo interaction. The Ce-based CeM_xX_{4-x} compounds with tetragonal $BaAl_4$-type structure are model cases for this behavior as here, by changing the chemical composition or applying pressure, magnetic as well as nonmagnetic ground states can be obtained.[1–3] Their unit cell consists of a body-centered arrangement of Ce atoms in which the M and X ions occupy the remaining sites more or less randomly (see Fig. 1). In the stoichiometric compounds with $x = 1$, this atomic disorder can be removed by formation of a $BaNiSn_3$-type structure. This structure is a derivative of the $BaAl_4$ structure but has no inversion center due to the sequence of ordered Ce-X(1)-X(2)-M layers (see Fig. 1).

The recently discovered unconventional superconductivity in the noncentrosymmetric $CeMSi_3$ and $CeMGe_3$ (M = Co,Rh,Ir) has intensified the efforts to investigate the ground state of the related $CeMX_3$ compounds with M = Cu,Ni,Au,Pd,Pt and X = Ga,Al.[4] $CeAuGa_3$, $CeNiGa_3$, and $CePdGa_3$ order antiferromagnetically at 2.4, 1, and 5.5 K, respectively,[5–7] while $CePtGa_3$ shows a spin-glass-type behavior.[8] All these compounds, in addition to their magnetic ordering, exhibit moderate heavy-fermion behavior. However, for several of them conflicting reports about their magnetic behavior have appeared in the literature, in particular for samples with composition deviating from the stoichiometric $x = 1$ composition.

A model case for this aspect is the $CeCuGa_3$ alloy. The first report on $CeCu_xGa_{4-x}$ compounds suggested ferromagnetic ordering of $CeCuGa_3$ at 3.5 K.[9] Studies on samples with varying Cu content, away from the stoichiometric composition, later indicated that this order is stabilized by decreasing x.[10–12] Mentink *et al.*[13] and Sampathkumaran and Das,[11] on the other hand, suggested that $CeCuGa_3$ is paramagnetic down to 0.4 K. A detailed investigation of polycrystalline $CeCuGa_3$ reveals Kondo-lattice behavior with magnetic ordering at 1.9 K suggested to be antiferromagnetic.[14] This was later supported by susceptibility measurements by Aoyama *et al.*[15,16] reporting a higher transition temperature of 4 K. From neutron-diffraction experiments on a single crystal (grown using the Czochralski method),[17] an incommensurate magnetic structure at 1.25 K was inferred with a propagation vector Q = (0.176,0.176,0). The magnetic scattering intensity extended up to 4 K. In addition, a broad, somewhat ill-defined specific-heat anomaly was observed between 1.5 and 4 K, whereas in polycrystals with a reduced Cu content of $x = 0.5$ a mean-field-like specific-heat anomaly was found.[11]

In view of these conflicting reports on the type of magnetic ordering and in order to study the magnetic properties more precisely, we have grown single crystals of $CeCuGa_3$ from Ga flux and investigated the anisotropic magnetic properties with measurements of the ac and dc magnetization, specific heat, and electrical resistivity.

II. EXPERIMENTAL DETAILS

Single crystals of $CeCuGa_3$ and $LaCuGa_3$ were grown by the flux method using Ga as flux. The starting materials were high-purity La and Ce (99.95%), Cu (99.99%), and Ga (99.999%). Stoichiometric amounts of the constituents with excess of Ga (1:25) were put into an alumina crucible and sealed in an evacuated quartz ampoule. The ampoule was heated to 1050 °C over a period of 24 h and held at that temperature for another 24 h for proper homogenization. The furnace was then cooled down to 400 °C at a rate of 1 °C/h followed by fast cooling to room temperature. The crystals were separated from the flux by centrifuging. Energy-dispersive x-ray analysis (EDAX) was performed on all crystals to identify their phase purity. The EDAX results showed 3% to 6% excess of Ga, which is attributed to the Ga flux used. X-ray powder diffraction patterns of all the compounds were recorded by powdering a small piece of single crystal (x-ray

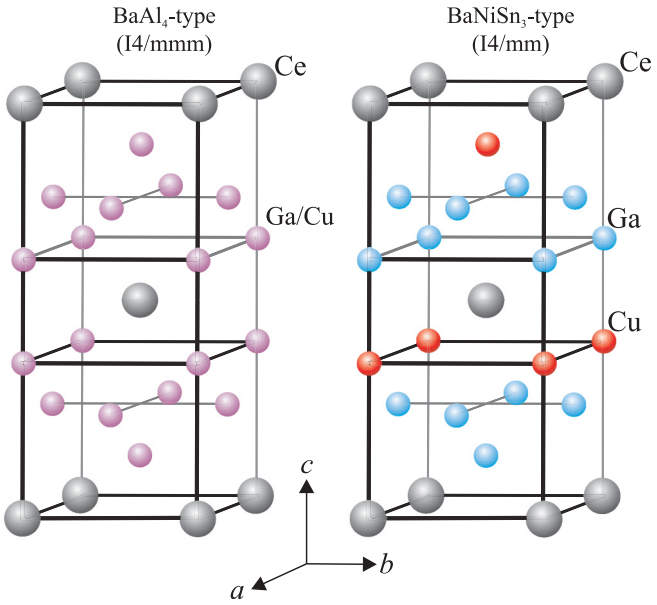

FIG. 1. (Color online) Two possible tetragonal crystal structures of $R\mathrm{Cu}_x\mathrm{Ga}_{4-x}$. If Cu and Ga occupy the 4*d* and 4*e* sites randomly, the BaAl_4 structure is adopted. For the stoichiometric compound $x = 1$ the Cu and Ga ions can order, resulting in the related noncentrosymmetric BaNiSn_3-type structure.

powder diffractometer STOE STADI P, Cu radiation). The single-crystal x-ray diffraction data sets were collected on an imaging-plate diffractometer system (STOE IPDS II, Mo $K\alpha$ radiation). The programs FULLPROF (Ref. 18) and SHELXL (Ref. 19) were used for a Rietveld analysis and structure refinement, respectively. The magnetic measurements were performed using a superconducting quantum interference device magnetometer from Quantum Design. The specific heat and resistivity were measured with a physical property measurement system from Quantum Design.

III. EXPERIMENTAL RESULTS

A. Crystal structure

$R\mathrm{CuGa}_3$ compounds crystallize in tetragonal derivatives of the BaAl_4 structure type (space group $I4/mmm$).[20] Depending on the degree of Cu-Ga order, these are mainly the BaAl_4, disordered $\mathrm{ThCr}_2\mathrm{Si}_2$ ($I4/mmm$), or noncentrosymmetric BaNiSn_3 ($I4mm$) structures (see Fig. 1). Powder diffraction cannot distinguish between these structure types but provides the tetragonal lattice parameters, which are for our LaCuGa_3 samples $a = 4.320(2)$ Å and $c = 10.436(2)$ Å and for CeCuGa_3 $a = 4.2729(2)$ Å and $c = 10.4359(4)$ Å. Together with the EDAX results, the lattice parameters show that the grown $\mathrm{CeCu}_x\mathrm{Ga}_{4-x}$ single crystals are, indeed, very close to the stoichiometric compound with $x = 1$.[9,10] The lattice parameter *a* decreases and *c* increases as we move from La to Ce. Overall, the unit-cell volume shrinks as expected from the lanthanide contraction. The c/a ratio is ≈2.4 for both compounds, indicating significant structural anisotropy. This is also reflected by the distance between adjacent Ce atoms, which is, at 4.2729(2) Å within the (*a*,*b*) plane, much shorter than the interplane distance of 6.0296(3) Å. Single-crystal

TABLE I. Comparative refinements for the average structure of CeCuGa_3.

Space group	R1	wR2	Goodness of fit	Parameters
*I*4/*mmm*	0.0224	0.0399	1.399	9
*I*4*mm*	0.0250	0.0475	1.317	15

x-ray diffraction has been used to resolve the structure type. In particular, we looked for a breakdown of the inversion symmetry by comparing refinement results from different models and analyzing the Flack parameter.[21] As this parameter is not significantly enhanced in the noncentrosymmetric *I*4/*mmm* model, we conclude that our single crystals adopt a BaAl_4 (or disordered $\mathrm{ThCr}_2\mathrm{Si}_2$) structure. Moreover, the refinement in the centrosymmetric space group *I*4/*mmm* gives the best agreement factors (R1 and wR2), with the smallest number of parameters (Table I). In addition, weak satellite Bragg peaks (1/1000 of the main peaks) have been observed that point to a modulation of the structure (Fig. 2). These satellite reflections were measured with a tube voltage of 30 kV, ruling out the presence of $\lambda/2$ radiation. A similar observation was made by Martin *et al.*,[17] with a modulation vector of (0.137,0.137,0), and attributed to a tendency towards an ordering of the Cu-Ga ions or a nearby structural transition. The modulation vector of our CeCuGa_3 samples is different from the literature and can in first approximation be written as (0,0,1/3), although it contains a small component in the a^* reciprocal direction, indicating a possible slight orthorhombic distortion of the lattice. Very weak third-order satellite reflections are present where reflections are otherwise forbidden from the body-centered lattice type. We also observe some diffuse scattering between the main reflections and the satellites along the c^* direction. A detailed description of the modulation in CeCuGa_3 will be given elsewhere.

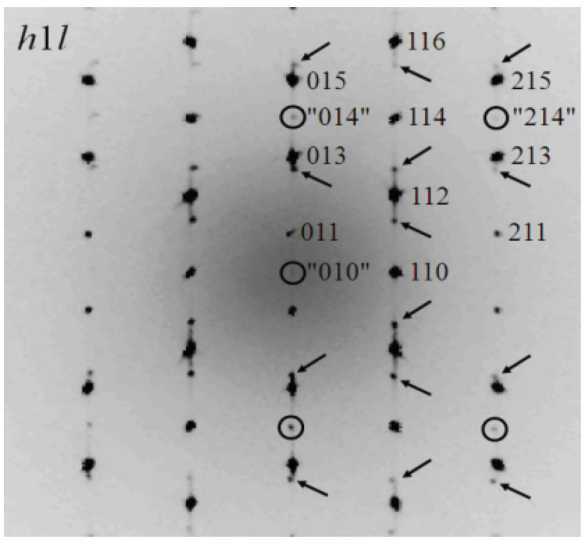

FIG. 2. Reconstruction of the *h*1*l* plane of the reciprocal space from single-crystal x-ray diffraction data. The arrows are pointing to the first- and second-order satellite reflections. The circles show the third-order satellites on the positions of forbidden reflections from the body-centered lattice.

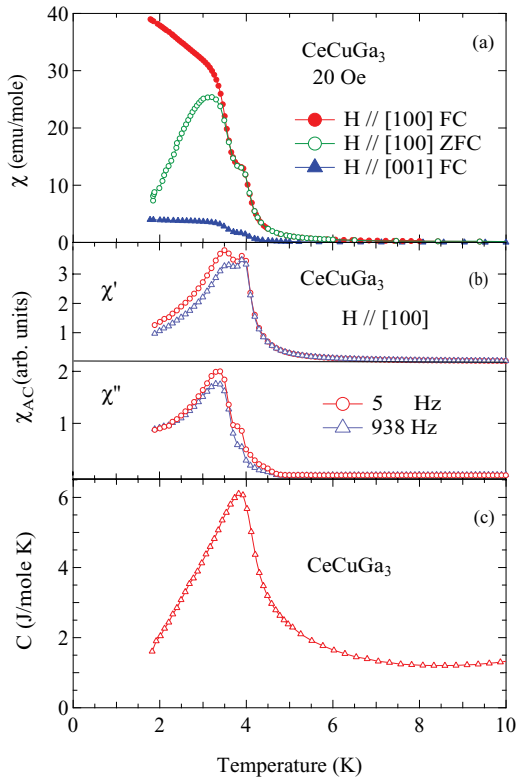

FIG. 3. (Color online) (a) Magnetic susceptibility of $CeCuGa_3$ under zero-field-cooled (ZFC) and field-cooled (FC) conditions for $H \parallel [100]$ and under FC condition for $H \parallel [001]$ as a function of temperature. (b) ac susceptibility with $H \parallel [100]$ and at frequencies of 5 and 938 Hz. (c) Low-temperature specific heat of $CeCuGa_3$ showing the anomaly at the magnetic phase transition.

B. Ferromagnetic ordering below 4 K

Figure 3 shows the low-temperature dc and ac susceptibilities, $\chi_{dc} = M/H$ measured in a magnetic field $H = 20$ Oe and χ_{ac}, and the specific heat C of $CeCuGa_3$. The data consistently indicate that $CeCuGa_3$ orders ferromagnetically at $T_C \approx 4.2$ K with the ab plane as the easy plane of magnetization; see Fig. 3(a). The zero-field-cooled (ZFC) and field-cooled (FC) measurements of χ_{dc} for $H \parallel [100]$, displayed in Fig. 3(a), demonstrate that with decreasing T, χ_{dc} reveals a Curie-Weiss-like increase followed by a kink at T_C. At $T < T_C$, the FC χ_{dc} continues to rise down to the lowest measured temperature of 1.8 K. The splitting of the ZFC and FC curves below T_C is in agreement with the expected behavior for a ferromagnet with domain-wall pinning which is enforced by the high magnetocrystalline anisotropy, i.e., $\chi_{dc}^{[100]}/\chi_{dc}^{[001]} \approx 8$ at $T = 2$ K; cf. Fig. 3(a). An unusual feature of the χ_{dc} measurements is the appearance of a shoulder at temperatures above the bifurcation of the ZFC and FC curves for both field directions. This feature was observed for several samples prepared independently.

To further investigate this anomaly, the ac susceptibility was measured at two frequencies of 5 and 938 Hz with $H \parallel [100]$ [see Fig. 3(b)]. In the real part of the ac susceptibility χ'_{ac}, two clear peaks are visible at ≈3.5 and ≈4 K. The imaginary part χ''_{ac} exhibits a peak and shoulder at the corresponding temperatures, indicating enhanced energy losses typical for thermodynamic phase or glass transitions. At the higher frequency of 938 Hz, the high-temperature peak in χ'_{ac} remains unaltered but the intensity of the low-temperature peak is reduced and its position seems to be shifted towards higher temperatures compared to the 5 Hz data. This frequency dependence might suggest the onset of spin-glass behavior out of the ordered state towards lower temperatures. However, as the peaks in χ''_{ac} do not show such a dependence the shift in χ'_{ac} is most probably an artifact caused by the rising edge of the larger high-temperature peak in χ'_{ac}.

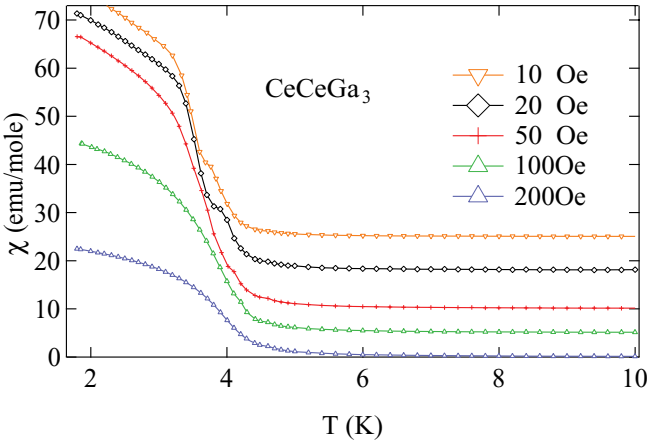

FIG. 4. (Color online) The susceptibility $\chi = M/H$ of $CeCuGa_3$ for $H \parallel [100]$ as a function of T in low magnetic fields. The curves are shifted with respect to one another for a better readability.

The specific heat of $CeCuGa_3$ is shown in Fig. 3(c) for comparison with the magnetic measurements. $C(T)$ shows a well-defined, rather sharp anomaly at the onset of the high-temperature shoulder in $\chi(T)$, which we therefore have taken as T_C. The size of the anomaly confirms bulk magnetic ordering. The specific heat does not show any feature corresponding to the low-temperature peak of $\chi_{ac}(T)$ and the ZFC $\chi(T)$ for $H \,||\, [100]$.

A systematic investigation of the field dependence of the $\chi(T) = M(T)/H$ at the double-step transition (Fig. 4) shows that the low-temperature shoulder shifts with field and eventually disappears at $H \approx 100$ Oe. A hysteresis loop $M(H)$ measured at 2 K for $H \,||\, [100]$ does not show any signs of the anomaly (Fig. 5). Magnetic isotherms of $CeCuGa_3$ also measured at 2 K with field applied along the [100] and [001] directions are displayed in Fig. 6 and reflect the strong magnetic anisotropy. From the high-field data at $H = 50$ kOe along the easy direction, we estimate a saturation moment of $M_s \approx 1.4\mu_B$/Ce. The magnetization with field along the hard axis, $H \parallel [001]$, undergoes a small jump at low fields and then increases slowly with H.

C. Crystal-electric-field effects

The inverse magnetic susceptibility χ_{dc}^{-1} of $CeCuGa_3$ in the paramagnetic state is shown in Fig. 7. A fit of a modified Curie-Weiss law for $T > 70$ K to the data for $H \parallel [100]$ and [001] (not shown) yields the effective moment μ_{eff}, the Curie temperature θ_P, and the temperature-independent susceptibilities χ_0 of $2.5\mu_B$/Ce and $2.51\mu_B$/Ce, 19 and −93 K and -10^{-4} and -7×10^{-5} emu/mol, respectively. The

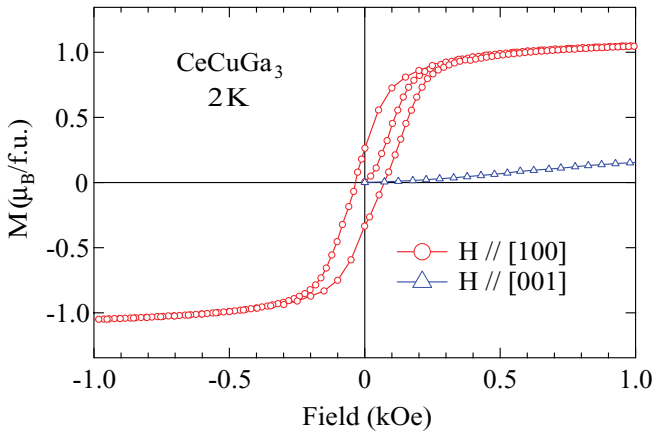

FIG. 5. (Color online) Magnetic hysteresis loop $M(H)$ of $CeCuGa_3$ measured at 2 K for H || [100]. The low-field (M) for H || [001] is also shown.

effective moments are close to the theoretically expected value for free Ce^{3+} ions ($2.54\mu_B$/Ce). The polycrystalline average of $\theta_P \approx -18.3$ K seems at first sight to be inconsistent with a ferromagnetic ground state. It has, however, taken into account that at lower temperatures the crystal electric field acting on the Ce ions lifts the degeneracy of the Hund's rule $4f$ ground-state multiplet $^2F_{5/2}$, leading to distinct deviations from the Curie-Weiss behavior below 70 K. A CEF calculation was done to obtain fits to the χ_{dc}^{-1} data for the whole temperature range 4–330 K. The site symmetry of the Ce atoms in the $CeCuGa_3$ unit cell is supposed to be tetragonal (point symmetry C_{4v}). The corresponding CEF Hamiltonian is given by

$$\mathcal{H}_{CEF} = B_2^0 O_2^0 + B_4^0 O_4^0 + B_4^4 O_4^4, \tag{1}$$

where B_ℓ^m and O_ℓ^m are the CEF parameters and the Stevens operators, respectively.[22,23] The CEF susceptibility is given by

$$\chi_{CEFi} = N(g_J\mu_B)^2 \frac{1}{Z}\left(\sum_{m\neq n} |\langle m|J_i|n\rangle|^2 \frac{1-e^{-\beta\Delta_{m,n}}}{\Delta_{m,n}} e^{-\beta E_n} + \sum_n |\langle n|J_i|n\rangle|^2 \beta e^{-\beta E_n}\right), \tag{2}$$

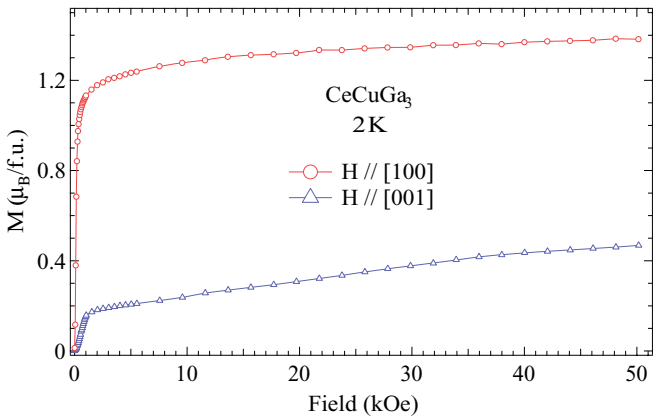

FIG. 6. (Color online) Magnetic isotherms of $CeCuGa_3$ at 2 K with field applied along the [100] and [001] directions.

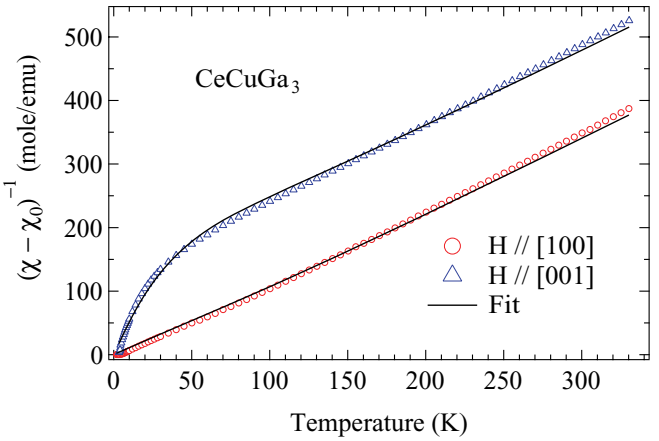

FIG. 7. (Color online) The inverse dc susceptibility of $CeCuGa_3$ after subtraction of the temperature-independent electronic contribution, $(\chi - \chi_0)^{-1}$, as a function of T for $H \parallel$ [100] and [001]. The black lines are fits to the crystal-electric-field (CEF) model described in the text.

where g_J is the Landé g factor, and E_n and $|n\rangle$ are the nth eigenvalue and eigenfunction, respectively. J_i ($i = x$, y, and z) are the components of the angular momentum, and $\Delta_{m,n} = E_n - E_m$, $Z = \sum_n e^{-\beta E_n}$, and $\beta = 1/k_B T$. The magnetic susceptibility including the molecular field constant λ_i is given by

$$\chi_i^{-1} = \chi_{CEFi}^{-1} - \lambda_i. \tag{3}$$

The CEF fits to the inverse susceptibility data $(\chi - \chi_0)^{-1}$ vs T are shown in Fig. 7. The resulting CEF parameters are $B_2^0 = 11.0$ K, $B_4^0 = 0.127$ K, and $B_4^4 = -3.0$ K with molecular field constants $\lambda^{[100]} = 1.46$ mol/emu and $\lambda^{[001]} = -1.9$ mol/emu, respectively, for $H \parallel$ [100] and [001]. The positive value of the dominating CEF parameter B_2^0 is consistent with the ab plane as the easy plane of magnetization. The CEF-split ground-state multiplet $^2F_{5/2}$ of Ce^{3+} ions in $CeCuGa_3$ can thus be described by three doublets with excitation energies of $\Delta_1 = 50$ K and $\Delta_2 = 228$ K.

Figure 8(a) shows the specific heat of $CeCuGa_3$ and its nonmagnetic analog $LaCuGa_3$ plotted as C/T vs T. The electronic contribution to the specific heat is estimated by extrapolating the "high-temperature" T^2 dependence of C/T observed between 12 and 25 K to $T = 0$ results in a Sommerfeld coefficient $\gamma \approx 20$ mJ/mol K^2 [inset of Fig. 8(a)]. This value is much smaller than that of 150 mJ/mol K^2 reported by Martin *et al.*[14] for the antiferromagnetic $CeCuGa_3$. The magnetic contribution C_{4f} to the specific heat [Fig. 8(b)] was determined from the $C(T)$ measurements by subtracting the phonon contribution estimated from the $C(T)$ of $LaCuGa_3$ and the electronic contribution $\gamma(T)$. The CEF contribution to C with the CEF parameters extracted from the susceptibility measurements is shown in Fig. 8(b). The good agreement with the measured C_{4f} data confirms our calculated CEF level scheme and indicates that the broad high-temperature peak represents a Schottky anomaly due to CEF excitations.

The calculated magnetic entropy S_{4f} is shown in the inset of Fig. 8(b). The magnetic entropy of the doublet ground state $R \ln 2$ is reached slightly above T_C. This points to a local-moment ferromagnet with only weak Kondo interaction, as corroborated by the large ordered magnetic moment and

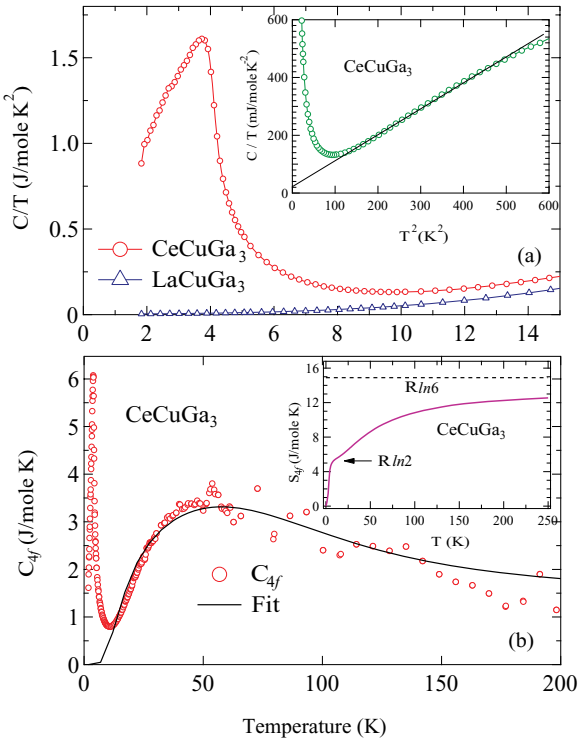

FIG. 8. (Color online) (a) The specific heat of $CeCuGa_3$ and $LaCuGa_3$ plotted as C/T vs T. The inset shows C/T as a function of T^2. The linear fit was used to extract the Sommerfeld constant. (b) The $4f$ contribution to the specific heat of $CeCuGa_3$ with a fit to the Schottky anomaly as described in the text. The inset shows the calculated $4f$ contribution to the entropy.

the clear plateau of $S_{4f}(T)$ at $R \ln 2$ just above T_c. The total magnetic entropy at 250 K is close to $R \ln 6$.

Finally the resistivity $\rho(T)$ of $CeCuGa_3$ is displayed in Fig. 9. With decreasing T, $\rho(T)$ exhibits a monotonic decrease followed by a leveling off around 10 K and a drop at the ordering temperature of 4 K (see inset of Fig. 9). These two latter features are attributed to a maximum of scattering by

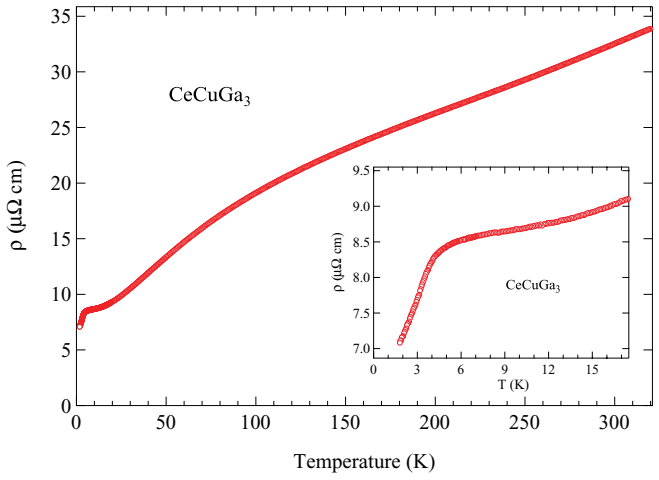

FIG. 9. (Color online) Resistivity of $CeCuGa_3$ $\rho(T)$ and its counterpart $LaCuGa_3$ without $4f$ electrons $\rho_{La}(T)$ which was used to estimate the magnetic contribution $\rho_{mag} \approx \rho - \rho_{La}$. The inset shows the low-temperature resistivity of $CeCuGa_3$.

magnetic fluctuations at T_C. Hence no clear indication of a Kondo effect can be inferred from the $\rho(T)$ data. The nonlinear decrease of $\rho(T)$ arises from a broad hump in $\rho(T)$ between 50 and 100 K which can be attributed to scattering from crystal-field excitations.[24] This assignment is supported by a comparison to $LaCuGa_3$ which displays an almost linear T dependence of $\rho(T)$ (not shown).

IV. DISCUSSION

Our measurements demonstrate that $CeCuGa_3$ has a ferromagnetic ground state if it adopts the centrosymmetric $BaAl_4$ structure. Its transition temperature matches the range of previously published measurements of $CeCu_xGa_{4-x}$. According to the published structure investigations, all ferromagnetic alloys crystallize in the centrosymmetric $BaAl_4$-type structure. The examples for antiferromagnetic or incommensurate magnetic order reported so far have a Cu concentration of $x \approx 1$ and adopt the noncentrosymmetric $BaNiSn_3$-type structure. At higher Cu contents, for $1 < x < 1.5$, no long-range magnetic order could be observed down to 0.4 K.

As for $x = 1$ different structural modifications can coexist, depending on the degree of atomic order, it is conceivable that here multiple magnetic transitions occur and, due to the frustration caused by the competing interactions, glasslike behavior might appear. In this context, the double-step transition in our magnetization measurements and the superstructure peaks seen in the x-ray diffraction studies can be interpreted as first signs towards a partially ordered $BaNiSn_3$ structure which enhances the antiferromagnetic correlations. This additional contribution is, however, very small because in the specific heat no additional transitions could be identified. In contrast, Martin *et al.*[17] reported more pronounced superstructure peaks and an unusual very broad anomaly in the specific heat that might perhaps be assigned to two different transitions at $\approx$4 and $\approx$2 K, respectively. At the lower temperature of $\simeq$2 K, they found the onset of the aforementioned, incommensurable, long-range magnetic order.

The magnetic entropy as well as the Sommerfeld coefficient of $CeCuGa_3$ with the $BaNiSn_3$ or $BaAl_4$ structure differ considerably from each other. While our measurements point to weak Kondo interactions (if present at all), Martin *et al.*[14] and Aoyama *et al.*[15] found a moderately heavy-fermion behavior with a clear Kondo-like minimum in the resistivity $\rho(T)$. Since the Kondo effect arises from a local interaction between the $4f$ electrons and the conduction-band electrons this difference has to originate from differences in the immediate environment of the Ce^{3+} ions. If in $CeCu_xGa_{4-x}$ the Cu concentration is further increased long-range magnetic order vanishes. Sampathkumaran and Das[10] observed a concomitant enhancement of the Kondo temperature. The border to the magnetic order in $CeCu_xGa_{4-x}$ and most of the other aforementioned CeM_xX_{4-x} alloys is close to $x \approx 1$, with the prospect of searching for quantum phase transitions.

Our estimated CEF parameters are similar to those published by Oe *et al.*[12] for ferromagnetic $CeCu_{0.8}Ga_{3.2}$. The magnetic behavior, in particular the anisotropy and the saturation moment, can be well explained by the CEF splitting. To our knowledge there exists no detailed investigation of the CEF level scheme of $CeCuGa_3$ with $BaNiSn_3$ structure.

V. CONCLUSION

The magnetic behavior of single-crystalline $CeCuGa_3$ has been studied. Depending on the Cu-Ga disorder the compound can adopt a tetragonal structure with ($BaAl_4$) or without ($BaNiSn_3$) inversion symmetry. The magnetic properties of $CeCuGa_3$ or, more generally, $CeCu_xGa_{4-x}$ sensitively depend on the environment of the Ce^{3+} ions. If the composition is shifted away from the stoichiometric limit $x = 1$, site disorder cannot be avoided and ferromagnetic ground states appear. In contrast to the noncentrosymmetric $CeCuGa_3$ without Cu-Ga site disorder, in the ferromagnetic compound only weak Kondo interactions could be observed. The magnetic anisotropy and the saturation moment correspond to the crystal-electric-field splitting of the Hund's rule $4f$ ground-state multiplet. Although $CeCuGa_3$ seems to be close to the onset of magnetic order, so far no clear signs of quantum critical behavior or unconventional superconductivity could be found. Future investigations have to verify whether pressure can suppress the magnetic order and cause deviations from Fermi-liquid behavior to appear.

ACKNOWLEDGMENTS

We thank M. Merz for fruitful discussions. D.A.J. acknowledges financial support by a postdoctoral fellowship of the Karlsruhe Institute of Technology. Part of this work was supported by the Deutsche Forschungsgemeinschaft through the Research Unit FOR 960.

[1] Y. Grin, P. Rogl, K. Hiebl, F. Wagner, and H. Noël, J. Solid State Chem. **70**, 168 (1987).
[2] H. Flandorfer, P. Rogl, E. Bauer, H. Michor, R. Hatzl, E. Gratz, and C. Godart, J. Phys.: Condens. Matter **8**, 2365 (1996).
[3] V. Fritsch and H. v. Löhneysen, J. Phys.: Conf. Ser. **150**, 042033 (2009).
[4] N. Kimura and I. Bonalde, in *Non-Centrosymmetric Superconductors: Introduction and Overview*, edited by E. Bauer and M. Sigrist, Lecture Notes in Physics Vol. 847 (Springer-Verlag, Berlin, 2012), pp. 35–79.
[5] S. Mock, C. Pfleiderer, and H. v. Löhneysen, J. Low Temp. Phys. **115**, 1 (1999).
[6] R. J. Cava, A. P. Ramirez, H. Takagi, J. Krajewski, and W. F. Peck, J. Magn. Magn. Mater. **128**, 124 (1993).
[7] J. Kim and Y. S. Kwon, Physica B **378**, 833 (2006).
[8] J. Tang, K. A. Gschneidner, R. Caspary, and F. Steglich, Physica B **163**, 201 (1990).
[9] Y. N. Grin, K. Hiebl, P. Rogl, and H. Noël, J. Less-Common Met. **162**, 371 (1990).
[10] E. Sampathkumaran and I. Das, Solid State Commun. **81**, 901 (1992).
[11] E. V. Sampathkumaran and I. Das, J. Magn. Magn. Mater. **147**, L240 (1995).
[12] K. Oe, Y. Kawamura, T. Nishioka, H. Kato, M. Matsumura, and K. Kodama, J. Phys.: Conf. Ser. **200**, 012147 (2010).
[13] S. A. M. Mentink, N. M. Bos, B. J. van Rossum, G. J. Neuwenhuys, J. A. Mydosh, and K. H. J. Buschow, J. Appl. Phys. **73**, 6625 (1993).
[14] J. M. Martin, D. M. Paul, M. R. Lees, D. Warner, and E. Bauer, J. Magn. Magn. Mater. **159**, 223 (1996).
[15] S. Aoyama, H. Ido, T. Nishioka, and M. Kontani, Czech. J. Phys. **46**, 2069 (1996).
[16] M. Kontani, G. Motoyama, T. Nishioka, and K. Murase, Physica B **259–261**, 24 (1999).
[17] J. M. Martin, M. R. Lees, D. M. Paul, P. Dai, C. Ritter, and Y. J. Bi, Phys. Rev. B **57**, 7419 (1998).
[18] J. Rodrigues-Carvajal, Physica B **192**, 55 (1992).
[19] M. Sheldrick, SHELX97, Universität Göttingen, Germany, 1997.
[20] E. Parthé, B. Chabot, H. F. Braun, and N. Engel, Acta Crystallogr., Sect. B **39**, 588 (1983).
[21] H. D. Flack, Acta Crystallogr., Sect. A **39**, 876 (1983).
[22] K. W. H. Stevens, Proc. Phys. Soc., London, Sect. A **65**, 209 (1952).
[23] M. T. Hutchings, in *Solid State Physics: Advances in Research and Applications*, edited by F. Seitz and B. Turnbull (Academic, New York, 1965), Vol. 16, p. 227.
[24] B. Cornut and B. Coqblin, Phys. Rev. B **5**, 4541 (1972).